

POAR: Towards Open-World Pedestrian Attribute Recognition

Yue Zhang, Suchen Wang, Shichao Kan, Zhenyu Weng,
Yigang Cen, *Member, IEEE*, Yap-peng Tan, *Fellow, IEEE*,

Abstract—Pedestrian attribute recognition (PAR) aims to predict the attributes of a target pedestrian in a surveillance system. Existing methods address the PAR problem by training a multi-label classifier with predefined attribute classes. However, it is impossible to exhaust all pedestrian attributes in the real world. To tackle this problem, we develop a novel pedestrian open-attribute recognition (POAR) framework. Our key idea is to formulate the POAR problem as an image-text search problem. We design a Transformer-based image encoder with a masking strategy. A set of attribute tokens are introduced to focus on specific pedestrian parts (e.g., head, upper body, lower body, feet, etc.) and encode corresponding attributes into visual embeddings. Each attribute category is described as a natural language sentence and encoded by the text encoder. Then, we compute the similarity between the visual and text embeddings of attributes to find the best attribute descriptions for the input images. Different from existing methods that learn a specific classifier for each attribute category, we model the pedestrian at a part-level and explore the searching method to handle the unseen attributes. Finally, a many-to-many contrastive (MTMC) loss with masked tokens is proposed to train the network since a pedestrian image can comprise multiple attributes. Extensive experiments have been conducted on benchmark PAR datasets with an open-attribute setting. The results verified the effectiveness of the proposed POAR method, which can form a strong baseline for the POAR task.

Index Terms—Class, IEEEtran, L^AT_EX, paper, style, template, typesetting.

I. INTRODUCTION

PEDESTRIAN attribute recognition (PAR) aims to predict attributes of a target pedestrian, such as gender, age, clothing, accessories, etc. As the applications in person search [1; 2; 3] and scene understanding [4; 5] are getting

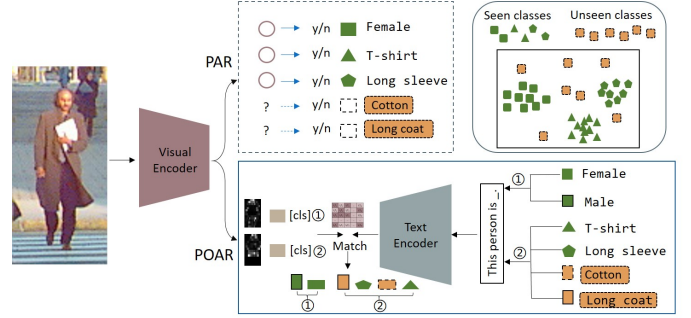


Fig. 1. The comparison of pedestrian attribute recognition (PAR) and pedestrian open-attribute recognition (POAR). The upper part shows the current PAR methods that are based on multi-label classification, where the attribute categories have been predefined. During the test, PAR methods cannot recognize new attributes that are beyond the predefined classes, such as cotton and long coat. The lower part presents our basic idea. We encode the images and attributes into a joint image-text feature space. Then, the attribute labels are determined based on the rank of the similarities between image embeddings and attribute embeddings.

more attention, PAR has become an active and significant research topic in computer vision. Existing methods such as global-local methods [6; 7; 8], attention methods [9; 8], textual semantic correlations methods [10; 11] address the PAR problem by training a multi-label classifier within a predetermined small attribute space. Thus they cannot be used to recognize attributes that do not exist in the predefined classes, such as “cotton” and “long coat” shown in Figure 1. In this work, we aim to explore how to handle the new attributes in open-world and discuss a new pedestrian open-attribute recognition (POAR) problem.

Pedestrian attribute recognition (PAR) aims to predict attributes of a target pedestrian, such as gender, age, clothing, accessories, etc. As the applications in person search [1; 2; 3] and scene understanding [4; 5] are getting more attention, PAR has become an active and significant research topic in computer vision. Existing methods such as global-local methods [6; 7; 8], attention methods [9; 8], textual semantic correlations methods [10; 11] address the PAR problem by training a multi-label classifier within a predetermined small attribute space. Thus they cannot be used to recognize attributes that do not exist in the predefined classes, such as “cotton” and “long coat” shown in Figure 1. In this work, we aim to explore how to handle the new attributes in open-world and discuss a new pedestrian open-attribute recognition (POAR) problem.

Recently, Radford *et al.* [12] proposed a CLIP (Contrastive Language-Image Pre-Training) method to model the similarity

Y. Zhang, and Y. Cen are with the School of Computer and Information Technology, Beijing Jiaotong University, Beijing 100044, China, and also with the Beijing Key Laboratory of Advanced Information Science and Network Technology, Beijing 100044, China (e-mail: 17112065@bjtu.edu.cn; ygcen@bjtu.edu.cn).

S. Wang and Z. Weng are with the School of Electrical and Electronic Engineering, Nanyang Technological University, 639798, Singapore (e-mail: suchen001@e.ntu.edu.sg; zhenyu.weng@ntu.edu.sg)

S. Kan is with the School of Computer Science and Engineering, Central South University, 410083, Changsha, Hunan, China (e-mail: kan-shichao@csu.edu.cn)

Y. Tan is with the School of Electrical and Electronic Engineering, Nanyang Technological University, 639798, Singapore (e-mail: cyptan@ntu.edu.sg)

Manuscript created October, 2022; This work was developed by the IEEE Publication Technology Department. This work is distributed under the L^AT_EX Project Public License (LPPL) (<http://www.latex-project.org/>) version 1.3. A copy of the LPPL, version 1.3, is included in the base L^AT_EX documentation of all distributions of L^AT_EX released 2003/12/01 or later. The opinions expressed here are entirely that of the author. No warranty is expressed or implied. User assumes all risk.

relationship between images and raw text. CLIP is trained in a task-agnostic setting and can be used to recognize general objects, such as airplane, bird, ocean, and so on. However, it cannot be directly used to recognize more fine-grained attributes, such as “upper stride”, “lower stripe”, “lower jeans”, “lower trousers”, in the PAR task. For the PAR, the challenge is that one pedestrian has multiple attributes and there is no corresponding location and scale information in the ground truth label set. To address this challenge, part-based [13] and attention mechanism [6] methods have been proposed to localize attributes and learn the attribute-specific regional features. However, these methods ignore the intra-region label conflicts, e.g., “long sleeve” and “short sleeve”. Zhao *et al.* [14] proposed a grouping attribute recognition method by dividing all labels into different groups and localizing regions corresponding to each group attribute based on the detection algorithm. However, the detection algorithm is attributed sensitive. Similarly, we also divide the whole attribute classes into multiple groups and each group corresponds to one visual region, as shown in Figure 1. But differently, we propose using masks to block out distracting and less informative regions and mask attribute tokens that do not relate to the attribute group. We localize attributes and learn their features based on token prediction with masks rather than detection.

Different from general PAR task that recognizes only the seen attributes in the training set, our POAR task allow the pedestrian attributes to expand beyond the seen attributes based on the interests and application needs. To address this challenge, we formulate the POAR problem as an image-text search problem, which is trained in a downstream attribute-agnostic manner under the supervision of natural language. Different from the CLIP that one image or object has only one class name, our method can use multiple attributes to describe one person in the POAR task. Using Figure 1 as an example, “male and long coat ” are used to describe this pedestrian. To address this problem, we propose a multiple attribute tokens ([ATT]) encoding method in the image encoding step. As shown in Figure 1, we divide the attributes into multiple groups and each group is encoded with an attribute token. The original image is encoded with multiple attribute tokens corresponding to multiple groups. Moreover, we block out less informative regions for the image token and filter out distracting attribute relations for the attribute tokens in each group. Based on the masking strategy and the many-to-many property, we propose a many-to-many contrastive (MTMC) loss with masked tokens to guide the parameter update of the network.

Our model is trained in an end-to-end manner. During training, we extract visual and text embeddings using the corresponding encoders. The similarity matrix of image-text pairs in a mini-batch can be calculated based on these embeddings. Then, the proposed many-to-many contrastive loss with masked embeddings is used to guide the learning of the model. During testing, attribute tokens of unseen attributes such as “cotton” and “long coat” in Figure 1 can be localized based on our model with the masking method. Then, features of those unseen attributes can be extracted from the localized regions. Meanwhile, text embeddings of those attributes can be

extracted using the text encoder. Finally, the attributes of one pedestrian can be recognized based on feature similarities of attribute tokens and text. Because the trained attribute encoder can be used to encode attributes which have not been seen during training, the proposed method can be used to recognize open attributes of the pedestrian in the open world.

Our contributions can be summarized as follows:

- We formulate the problem of pedestrian open-attribute recognition (POAR) and develop a simple yet effective method to address it.
- We propose a masking mechanism to address problems of multiple attribute localization and multiple tokens encoding in the POAR task. Furthermore, a many-to-many contrastive loss with masked tokens is proposed to train the network.
- Extensive experiments on benchmark datasets with an open-attribute setting have been conducted to demonstrate the effectiveness of the proposed method, which forms a strong baseline for the POAR task.

II. RELATED WORK

This work is related to pedestrian attribute recognition and open-world recognition. In this section, we review the existing methods on these topics.

A. Pedestrian Attribute Recognition

Pedestrian attribute recognition (PAR) has attracted increasing interest in person recognition [15; 16; 17; 18; 19] and scene understanding [17; 18; 19]. The mainstream methods address this problem by building a multi-label classifier based on CNN. To improve the recognition accuracy, global methods[20; 9], local methods[21], and global-local attention-based methods [22] are proposed. Nikolaos *et al.* [21] proposed an effective method to extract and aggregate visual attention masks across different scales. Tang *et al.* [6] proposed a flexible attribute localization module to learn attribute-specific regional features. These methods focused on domain-specific model designing. To use additional domain-specific guidance, M. Kalayeh *et al.* [23] used semantic segmentation methods to learn attention maps for accurate attribute prediction. Liu *et al.*[18] learned clothing attributes with additional landmark labels. Li *et al.* [11] proposed an image-conditioned masked language model to learn complex sample-level attribute correlations from the perspective of language modeling. Cheng *et al.* [10] proposed an additional textual modality to explore the textual semantic correlations from attribute annotations. These methods are trained on a predefined attribute set and used to recognize the same attributes, which limits the flexibility of these models. In our work, we build a pedestrian open-attribute recognition (POAR) model based on the CLIP [12] model to flexibly recognize both seen and unseen pedestrian attributes.

B. Open World Recognition

POAR problem is an open-world recognition (OWR) problem for pedestrian attributes. In classification, OWR is first proposed by Scheirer [24], which aims to discriminate known

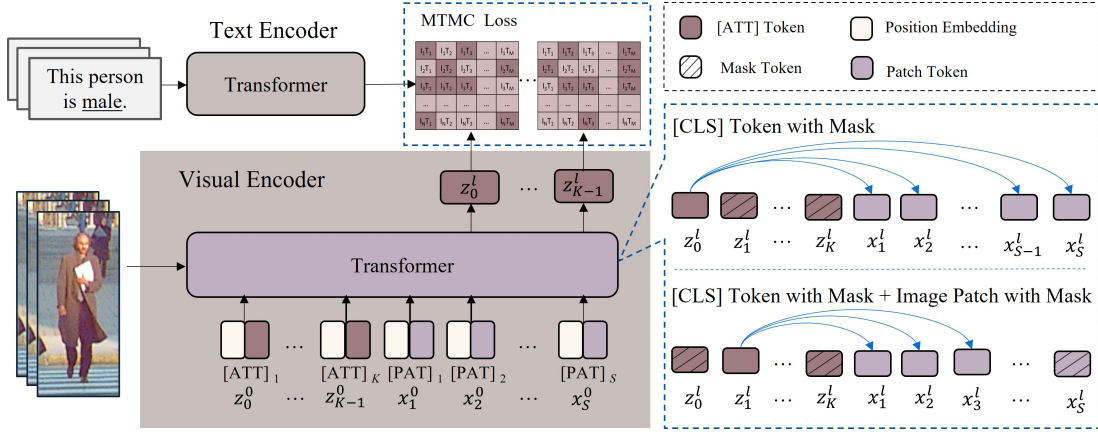


Fig. 2. The proposed POAR framework. The proposed model is designed for pedestrian open-attribution recognition. We evaluate the dot similarity of features from the image and text encoder and then determine the attributes of the pedestrian in the image.

from unknown samples as well as classify known ones. Latter, prototype-based method[25; 26], knowledge distillation method[27], and out-of-distribution detection method[28] become popular in image classification and object detection. Esmailpour *et al.* [28] used an extended model to generate candidate unknown class names for each test sample and compute a confidence score based on both the known class names and candidate unknown class names for zero-shot out-of-distribution detection. Oza *et al.* [29] proposed the class conditional auto-encoder to tackle open-set recognition, which includes closed-set training and open-set training stages. Gu *et al.* [27] adopted an image-text pre-trained model as a teaching model to supervise student detectors. Zhao *et al.*[30] unified the label space from the training of multiple datasets to improve the generalization ability of a model. In addition, some methods [31; 32] aligned region features and the pre-trained text embeddings in base categories to realize zero-shot detection. The CLIP model was proposed by Radford *et al.*[12], which performs task-agnostic training via natural language prompting. CLIP can realize zero-shot image recognition. However, CLIP is usually used to recognize general objects, such as airplane, bird, ocean, and so on. For fine-grained attribute recognition, such as attributes of a pedestrian and the granular features of birds, CLIP will fall short in most situations. In our work, we build a model for the recognition of pedestrian open attributes.

III. METHOD

In this section, we first define the pedestrian open-attribution recognition (POAR) problem. Then we introduce our POAR framework, as shown in Figure 2. Finally, we present the details of the loss function.

A. Pedestrian Open-Attribute Recognition

Pedestrian attribute recognition (PAR) aims to recognize the fine-grained attributes of a person (e.g., hairstyle, age, gender, etc.) from the given pedestrian image. The conventional PAR usually predetermines a set of pedestrian attributes and follows the close-set assumption during both the training and

test phases. Suppose we have M predetermined pedestrian attributes $\mathcal{A} = \{A_1, A_2, \dots, A_M\}$, e.g., A_1 = “long hair”, A_2 = “short hair”, etc. Then, given a labeled pedestrian dataset $\mathcal{D} = \{(I_i, \mathcal{A}_i)\}_{i=1}^N$, where each image $I_i \in \mathbb{R}^{H \times W \times 3}$ is annotated with a subset $\mathcal{A}_i \subset \mathcal{A}$ to denote the existing pedestrian attributes. The main objective of PAR is to learn a model to answer which pedestrian attributes from \mathcal{A} appear in the given image I .

Existing approaches [6; 7; 10] usually convert this to a multi-label classification problem. However, the pedestrian attributes in the real world are potentially unlimited. It is difficult to exhaust all of them in a predetermined attribute set and collect the corresponding pedestrian images. Unseen attributes are highly possible to exist in real applications, while existing classification-based methods [10; 11] are inherently incapable of handling this case. To address this issue, we introduce a pedestrian open-attribute recognition (POAR) problem in this work. Let $\mathcal{A}_u = \{A_{M+1}, A_{M+2}, \dots, A_{M+M_u}\}$ denote a set of extra attributes which are also of interest in the test phase but out of the predetermined attribute set \mathcal{A} . In POAR, we expect that the model can not only recognize the seen attributes from \mathcal{A} but also the unseen attributes from \mathcal{A}_u .

B. Framework

Overview. As shown in Figure 2, we use an image-text contrastive learning framework with an image encoder Φ_I and a text encoder Φ_T . The image encoder aims to process input images and derive the visual representation of various pedestrian attributes. Besides, we construct a set of text descriptions (e.g., “this person has long hair”, “this person is carrying backpack”, etc). We utilize the text encoder of CLIP to encode these attribute descriptions into text embeddings. Then, we compute the vision-text similarity to find the best-matched pedestrian attributes for the input images. Different from the original CLIP, one pedestrian may have more than one associated attribute, as shown in Figure 3. To train our model, we propose a many-to-many contrastive (MTMC) loss with masked tokens to handle the many-to-many relationships between the images and text descriptions. The details of each part are introduced below.

TABLE I
ATTRIBUTE LABELS OF THE PETA DATASET ARE CONVERTED TO SEQUENCE BY THE PROMPT.

ATTRIBUTES	KEY	PROMPT
Long, short	Hair	This person has {} hair.
Male, Female	Gender	This person is {}.
Less15, Less30, Less45, Less60, Larger60	Age	The age of this person is {} years old.
Backpack, MessengerBag, PlasticBags, Other, Nothing	Carry	This person is carrying {}.
Sunglasses, Hat, Muffler, Nothing	Accessory	This person is accessory {}.
LeatherShoes, Sandals, Sneaker, Shoes	Foot	This person is wearing {} in foot.
Casual, Formal, Jacket, Logo, ShortSleeve, Plaid, Stripe, Tshirt, VNeck, Other	Upperbody	This person is wearing {} in upper body.
Casual, Formal, Trousers, ShortSkirt, Shorts, Plaid, Jeans	Lowerbody	This person is wearing {} in lower body.

Image Encoding. The image encoding process is organized based on token prediction with Transformer as follows. First, the input image I is split into a sequence of non-overlapping small patches $\{P_0, P_1, \dots, P_{S-1}\}$, where $P_i \in \mathbb{R}^{r \times r \times 3}$ and $S = \frac{H}{r} \times \frac{W}{r}$. Then, each patch P_i is projected to an embedding vector $\mathbf{x}_i \in \mathbb{R}^D$ ([PAT]), where D denotes the feature dimension. Thus, we can obtain $\mathbf{X} = [\mathbf{x}_0, \mathbf{x}_1, \dots, \mathbf{x}_{S-1}] \in \mathbb{R}^{D \times S}$ with S patch embeddings. Inspired by [33; 12], we introduce K learnable attribute tokens $\mathbf{Z} = [\mathbf{z}_0, \mathbf{z}_1, \dots, \mathbf{z}_{K-1}] \in \mathbb{R}^{D \times K}$, where each attribute token $\mathbf{z}_k \in \mathbb{R}^D$ shares the same dimension as \mathbf{x}_i . For each patch embedding and each class token, we generate a corresponding position encoding $\mathbf{e}_j \in \mathbb{R}^D$, where $j \in \{0, 1, \dots, S + K - 1\}$. The input of the image encoder Φ_I is the concatenation of class tokens and patch embeddings combined with their positional embeddings $\mathbf{E} = [\mathbf{e}_0, \mathbf{e}_1, \dots, \mathbf{e}_{S+K-1}] \in \mathbb{R}^{D \times (S+K)}$, which is denoted as $\mathbf{V} = [\mathbf{Z}, \mathbf{X}] \oplus \mathbf{E}$, where $\mathbf{V} \in \mathbb{R}^{D \times (S+K)}$, $[\cdot]$ is the concatenate operation, and \oplus is the element-wise summation notation. The output of the image encoder Φ_I is the learned embeddings of class tokens, denoted as $\hat{\mathbf{Z}} \in \mathbb{R}^{D \times K}$. The above process is summarized as follows:

$$\hat{\mathbf{Z}} = \Phi_I(\mathbf{V}). \quad (1)$$

Text Encoding. The process of text encoding is formed based on the text encoder Φ_T transferred from the CLIP model. The input of the text encoder is the prompts of pedestrian attributes which are organized as follows. First, the attributes are divided into K groups based on the characteristics of pedestrians, as shown in Table I. Then, we format a prompt template for the attributes of each group. Finally, each prompt sentence is tokenized into an embedding using the Byte-Pair-Encoding method¹. Suppose that the maximum number of words in these sentences is L . Then, each sentence is tokenized into a vector $\mathbf{y}_i \in \mathbb{R}^L$. For the k -th group, we can obtain m sentence vector corresponding with m prompts in this group, denoted as $\mathbf{Y}^k = [\mathbf{y}_1^k, \mathbf{y}_2^k, \dots, \mathbf{y}_m^k] \in \mathbb{R}^{L \times m}$. The output of the text encoder Φ_T is the learned text embeddings $\hat{\mathbf{Y}}^k$ for the prompts of the k -th group. The above process can be defined as:

$$\hat{\mathbf{Y}}^k = \Phi_T(\mathbf{Y}^k), \quad (2)$$

where $\hat{\mathbf{Y}}^k \in \mathbb{R}^{D \times m}$.

Many-to-Many Contrastive Loss. For a mini-batch images $\{I_1, I_2, \dots, I_B\}$, we first extract their token embeddings $\hat{\mathbf{Z}}_b$

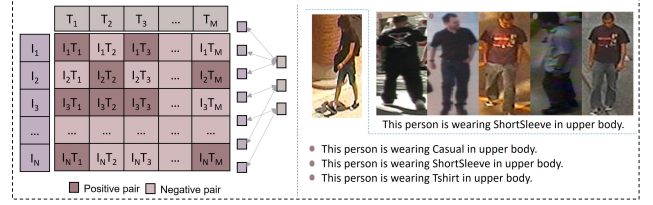


Fig. 3. Diagram of image-text relationship. The right part represents the many-to-many relationship between text and images.

and text embeddings $\hat{\mathbf{Y}}_b$ based on formulas (1) and (2), respectively. $\hat{\mathbf{Z}}_b$ and $\hat{\mathbf{Y}}_b$ are sets of token embeddings and text embeddings in all attribute groups related to the given mini-batch images, respectively. Different from the CLIP model which has a one-to-one relationship between image and text. In POAR, the image and text are involved in a many-to-many relationship, as shown in Figure 3. To effectively tackle this scenario, a loss function combined with visual-to-text and text-to-visual contrastive learning is proposed. The visual-to-text contrastive learning term is defined as follows:

$$\mathcal{L}_{v2t} = -\sum_{i=1}^v \sum_{j=1}^{t_i} \log \frac{\exp(\hat{\mathbf{z}}_i^T \hat{\mathbf{y}}_j^+ / \tau)}{\sum_{k=1}^t \exp(\hat{\mathbf{z}}_i^T \hat{\mathbf{y}}_k / \tau)}, \quad (3)$$

where τ is a temperature parameter, t_i is the number of positive text embeddings that have the same attribute label with $\hat{\mathbf{z}}_i$. v and t are the number of token embeddings and text embeddings, respectively. $\hat{\mathbf{z}}_i \in \hat{\mathbf{Z}}_b$, $\hat{\mathbf{y}}_j \in \hat{\mathbf{Y}}_b$, $\hat{\mathbf{y}}_j^+ \in \hat{\mathbf{Y}}_b$. $\hat{\mathbf{z}}_i$ and $\hat{\mathbf{y}}_j^+$ is a positive pair which means that they share the same attribute label. Similarly, the text-to-visual contrastive learning term is defined as follows:

$$\mathcal{L}_{t2v} = -\sum_{j=1}^t \sum_{i=1}^{v_j} \log \frac{\exp(\hat{\mathbf{y}}_j^T \hat{\mathbf{z}}_i^+ / \tau)}{\sum_{k=1}^v \exp(\hat{\mathbf{y}}_j^T \hat{\mathbf{z}}_k / \tau)}, \quad (4)$$

where v_j is the number of positive token embeddings that have the same attribute label with $\hat{\mathbf{y}}_j$. The final loss function is the combination of (3) and (4), as follows:

$$\mathcal{L} = \mathcal{L}_{v2t} + \mathcal{L}_{t2v}. \quad (5)$$

To this end, we have described the main framework of our POAR. To train the network, a masking strategy is introduced in the following section.

C. Encoder Networks and Mask Strategy

In this part, we present the details of the image encoder and our mask strategy for network training.

¹https://huggingface.co/transformers/v4.8.0/model_doc/clip.html

Image Encoder. The image encoder Φ_I is a stack of multi-layer Transformer blocks. The Transformer block is composed of layer norm (LN) layers [33], a multi-head self-attention (MSA) layer [33], and a multi-layer perceptron (MLP) network. In the multi-head self-attention layer, the attention weights of each attribute token are automatically calculated among all input tokens. Specifically, the attention weights between the k -th attribute token and the others can be written as

$$\text{Attn}_{\text{token}}(\mathbf{z}_k) = \text{softmax}\left(\frac{[\mathbf{z}_k^\top \cdot \mathbf{Z}, \mathbf{z}_k^\top \cdot \mathbf{X}]}{\sqrt{D}}\right). \quad (6)$$

We observe that the first term $\mathbf{z}_k^\top \mathbf{Z}$ often dominates the attention, making the module hardly find the true regions of interest from the input image. This shortcut learning often leads to overfitting and inferior results in our experiments. To address this issue, we mask out the self-attentions between the attribute tokens. We use this way to force them to independently extract useful visual information from the input image rather than simply relying on the information that has been extracted by the others. Specifically, we calculate the attention weight of the k -th attribute token as

$$\text{Attn}_{\text{mask}}(\mathbf{z}_k) = \text{softmax}\left(\frac{[\mathbf{z}_k^\top \cdot \mathbf{X}]}{\sqrt{D}}\right). \quad (7)$$

In our experiments, we observe that this technique leads to significant performance gain (Table IV). The mask strategy is described as follows.

In the PAR task, one key challenge is that a pedestrian can have multiple attributes and there is no corresponding location and scale information in the ground truth label set. We propose the above mask strategy to tackle this challenge. Specifically, we divide the whole attribute classes into multiple groups and each group ([ATT] token) corresponds to one visual region, we mask out regions ([PAT] token) that do not need to pay attention to. For example, the “hair” class token pays more attention to the head of the pedestrian and we block out regions on the lower part of the head region, the “upper body” class token pays more attention to the top part of the image and we block out the bottom part of the image, etc. Thus, the final attention can be calculated as follows

$$\text{Attn}_{\text{mask}}(\mathbf{z}_k^l) = \text{softmax}\left(\frac{\mathbf{z}_k^l \cdot \mathbf{X} + \varpi}{\sqrt{D}}\right), \quad (8)$$

where $\varpi \in \mathbb{R}^{1 \times S}$ is a mask vector with value $-\infty$ for the blocked image patches and 0 otherwise. Taking the “hair” class token, for example, the region of the head will be 0 and the remaining regions will be $-\infty$. The output of the self-attention unit is as follows:

$$\mathbf{F}^l = \text{Attn}_{\text{mask}}(\mathbf{Z}_k^{l-1}) \cdot \mathbf{V}^{l-1}, \quad (9)$$

where l is the layer index of the self-attention, $\mathbf{Z}^0 = \mathbf{Z}$, $\mathbf{V}^0 = \mathbf{V}$. The whole process of a Transformer block can be formulated as:

$$\hat{\mathbf{V}}^l = \text{MSA}(\text{LN}(\mathbf{V}^{l-1})) + \mathbf{V}^{l-1}, \quad (10)$$

$$\mathbf{V}^l = \text{MLP}(\text{LN}(\hat{\mathbf{V}}^l)) + \hat{\mathbf{V}}^l. \quad (11)$$

Contrastive Learning with Masked Tokens. It should be noted that our contrastive loss is computed based on all the token embeddings and attribute embeddings. The embeddings of those masked tokens are also used to compute the loss, which is because the contrastive loss computed with the masked embeddings will lead to more robust embedding learning.

IV. EXPERIMENTS

TABLE II

THE NUMBER OF ATTRIBUTE CLASSES IN THE TEST PHASE. SN AND UN REPRESENT THE NUMBER OF SEEN CLASSES AND UNSEEN CLASSES IN THE TEST SETS, RESPECTIVELY.

Source Domain	Target Domain					
	PETA		PA100K		RAPv1	
	SN	UN	SN	UN	SN	UN
PETA	35	0	10	16	14	37
PA100K	12	23	26	0	9	42
RAPv1	16	19	10	16	51	0

A. Datasets and Experimental Settings

Datasets and Evaluation Metrics. The proposed POAR method is evaluated on three benchmark datasets, i.e., PETA [34], RAPv1 [35], and PA-100K [9] with an open-attribute setting. The Recall@K and mA are used to evaluate the performance of our open-attribute recognition model. Our model is trained on one dataset and evaluated on the other two datasets.

Implementation Details. Our experiments are conducted based on the ViT-B/16 backbone networks which are stacked with 12 Transformer blocks. The input image size is set to 224×224 . The value of r is set to 16. and K is set to be 8, 8, and 11 in PETA, PA100K, and RAPv1 respectively. The learning rate is $5e^{-2}$ with a weight decay of 0.2. The model is trained from scratch with 100 epochs. The temperature τ in our contrastive loss is set to be 1. Data augmentation with random horizontal flip and random erasing are used during training.

B. Performance Comparison of POAR

We compare the performance of our method with the CLIP [12] and VTB [10] methods based on the image-to-text K -nearest neighbor retrieval idea. In Table II, SN and UN are the number of seen and unseen attributes used in the test sets, respectively. Performance comparison with the top-1 and top-2 recall rates are shown in Table III.

From Table III, we can see that the Recall@1 scores of our method are 1.7% and 8.6% higher than the CLIP method when the model is trained on the PETA dataset and evaluated on the PA100K and RAPv1 datasets, respectively. When the model is trained on the PA100K and evaluated on the PETA dataset, the recall@1 score of our method is 7.9% lower than the CLIP model. When the model is trained on the RAPv1 and evaluated on the PETA and PA100K datasets, the recall@1 scores of our method are 7.3% and 5.1% lower than the CLIP model. This

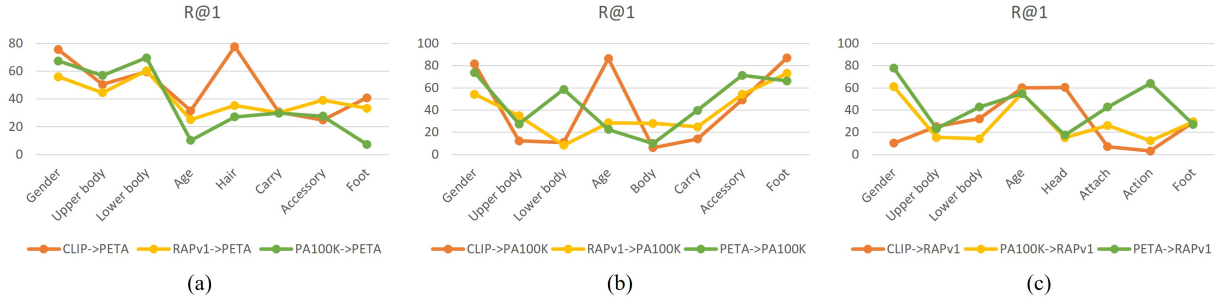


Fig. 4. Performance comparison of different groups ([ATT] tokens) by different methods based on the same experimental settings. (a), (b), and (c) represent the results on PETA, PA100K, and RAPv1 datasets, respectively.

TABLE III
PERFORMANCE COMPARISON OF POAR EXPERIMENTAL RESULTS. BLUE INDICATES THE MODEL IS TRAINED AND TESTED ON THE SAME DATASET.

Method	Source Domain	Target Domain					
		PETA		PA100k		RAPv1	
		R@1	R@2	R@1	R@2	R@1	R@2
CLIP*	—	50.2	75.7	43.4	65.9	33.6	56.5
VTB*	PA100K	31.4	62.2	26.9	62.2	24.2	50.7
Ours	PETA	87.6	96.0	45.1	73.5	42.2	68.6
Ours+CLIP	PETA	—	—	44.7	74.7	42.1	69.7
Ours	PA100K	42.3	76.2	83.3	92.6	39.4	63.6
Ours+CLIP	PA100K	50.9	77.5	—	—	39.4	64.5
Ours	RAPv1	42.9	72.5	38.3	62.6	75.8	88.8
Ours+CLIP	RAPv1	52.9	78.8	45.5	67.2	—	—



Fig. 5. The R@1 scores of seen and unseen attributes of each attribute token for the PA100K dataset.

is because the CLIP model is trained on 400 million image-text pairs which have a high probability to contain “age” and “hair” and other attributes, thus those unseen attributes defined in our experiments can be considered seen in the CLIP model. However, when we fuse the features of our model and the CLIP model, the highest performance for the POAR task can be obtained.

To analyze the details of the POAR performance, we show the performance comparison of each group of the CLIP model and the proposed POAR model in Figure 4. We can see that the CLIP model has higher recognition performance for attributes in “age” and “hair” groups, which has a high probability of being seen by the CLIP model during training. For attributes in the “upper body” group that has a low probability of being seen by the CLIP model, the recognition performance of our model is much higher than the CLIP model.

Furthermore, we compute the recognition performance of

TABLE IV
EVALUATION OF EACH COMPONENT ON THE PETA DATASET. SC REPRESENTS A SINGLE ATTRIBUTE TOKEN. MC REPRESENTS MULTIPLE ATTRIBUTE TOKENS. CM REPRESENTS AN ATTRIBUTE TOKEN THAT IS BLOCKED OUT WITH THE MASK. BLOCK REPRESENTS AN IMAGE PATCH THAT IS BLOCKED OUT WITH THE MASK.

SC	MC	CM	Block	mA	F1	R@1	R@2
✓				81.1	83.0	85.7	94.7
	✓			80.6	82.2	86.2	95.7
	✓	✓		81.0	83.0	86.4	95.7
	✓	✓	✓	83.1	84.4	87.6	96.0

TABLE V
OUR TEST RESULTS FOR DIFFERENT LOSS FUNCTIONS IN THE PETA DATASET. OTOC REPRESENTS THE ONE-TO-ONE CONTRASTIVE LOSS. MTMC REPRESENTS THE MANY-TO-MANY CONTRASTIVE LOSS.

OTOC	MTMC	mA	F1	R@1	R@2
✓		73.0	73.4	86.3	95.8
✓	✓	81.5	83.3	86.3	95.8
	✓	83.1	84.4	87.6	96.0

seen and unseen attributes in the PA100K dataset, respectively. Results are shown in Figure 5, we can see that the R@1 scores of seen attributes are much higher than unseen attributes for the “age” group. For the “upperbody” group, the R@1 scores of unseen attributes are much higher than the seen attributes, which indicates that our model generalizes better for unseen attributes in this group.

TABLE VI
RESULTS OF TEXT-TO-IMAGE RETRIEVAL ON DIFFERENT DATASETS. BLUE INDICATES THAT THE TRAIN SET AND TEST SET BELONG TO THE SAME DATASET.

Method	Source Domain	Target Domain								
		PETA			PA100K			RAPv1		
		R@1	R@5	R@10	R@1	R@5	R@10	R@1	R@5	R@10
POAR	PETA	90.3	100.0	100.0	38.5	57.7	61.5	35.3	52.9	62.8
POAR	PA100K	41.9	74.2	77.4	88.5	96.2	100.0	33.3	56.9	64.7
POAR	RAPv1	35.5	58.1	71.0	34.6	61.5	69.2	96.1	100.0	100.0

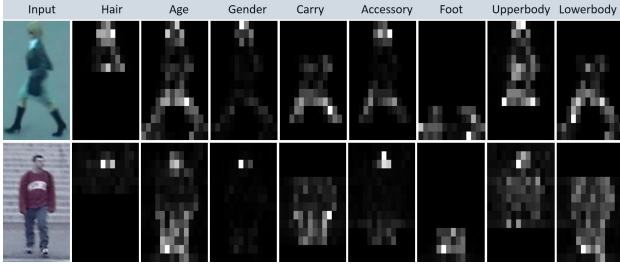


Fig. 6. The attention map of each class token on PETA dataset.

C. Ablation Study

Our ablation study is conducted on the PETA dataset using the close-set evaluation mechanism. Table IV shows the image-to-text retrieval performance of different components in our proposed method. Table V shows the image-to-text retrieval performance for different loss functions. The one-to-one loss function is performed by defining all attributes of one image to a paragraph description as text input. From Table IV, we can see that each component of the proposed method can contribute to the final performance gain. From Table V, we can see that the many-to-many loss function significantly improves the final performance.

D. Visualization of the Attention Maps

To show the effectiveness of the proposed masking method, we visualize the attention map of each attribute token on the PETA dataset, and the results are shown in Figure 6. In our method, we proposed a masking strategy to block out distract regions and mask the corresponding attribute tokens. From the attention map, we can see that each attribute token is independently responsible for a specific part of the body, which shows the effectiveness of the proposed masking method. For example, the attention maps of the second column concentrated on the “hair” part, and the attention maps of the third column concentrated on the whole body of a pedestrian which is related to the “age” of a person, etc.

E. Text-to-Image Retrieval Results

To show the generalization of our method, we also evaluate the text-to-image retrieval results. Each attribute sentence is encoded into a text embedding, and those text embeddings are used to retrieve similar images based on the attribute token embeddings, and the results are reported in Table VI. Compared

to the image-to-text retrieve performance of Table III, we can see that the text-to-image recognition task is more challenging than the image-to-text recognition task, which is mainly due to that the text embedding space is more sparse than the image embedding space.

F. Image-to-Text Retrieval Examples

In Figure 9, we visualize some image-to-text retrieval examples based on embeddings obtained using our proposed POAR method. The model was trained on the PETA dataset. Figure 7 and Figure 8 show examples tested on the PA100K and RAPv1 datasets, respectively. Attributes with the pink box are unseen attributes during training. We can see that there are a lot of unseen attributes in the test set and our model can effectively recognize those unseen attributes. Prompts with blue color indicate that the predicted text is inconsistent with the ground truth. We can see that the proposed model is difficult to recognize the age and direction of one person as shown in Figure 7 (ii) and (iii) on the PA100K dataset. On the RAPv1 dataset, the model has more difficulty in recognizing the hair and id. These examples show that there is still room for improvement to recognize pedestrian attributes in open-world scenarios. In our future work, we will continue to address these problems.

V. CONCLUSIONS

We have addressed the problem of pedestrian open-attribute recognition and proposed a novel method to tackle this problem. Our key idea is to formulate the POAR problem as an image-text search problem. Specifically, we proposed a multiple attribute tokens encoding method to encode image patches with attribute tokens. Then, a masking mechanism is devised to block out distracting image patches with less informative and mask attribute tokens that do not relate to the attribute group. Finally, a many-to-many contrastive loss function with masked tokens is developed to train the model. Experimental results on benchmark PAR datasets with an open-attribute setting show the effectiveness of the proposed method.

Limitations: One limitation of the work is that the text encoder is transferred from the CLIP, we will design a more effective attribute encoder in our future work. Another limitation is that the input of the framework is the detected pedestrian, future work could be focused on integrating pedestrian detection and POAR into a unified framework.

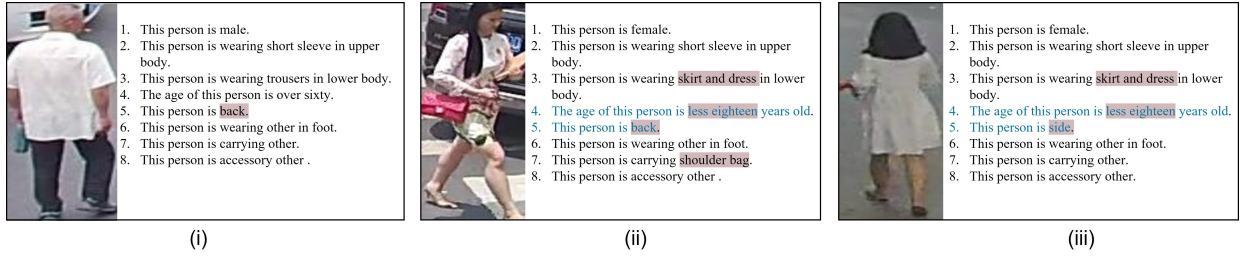


Fig. 7. Examples of image and text matching on the PA100K dataset.

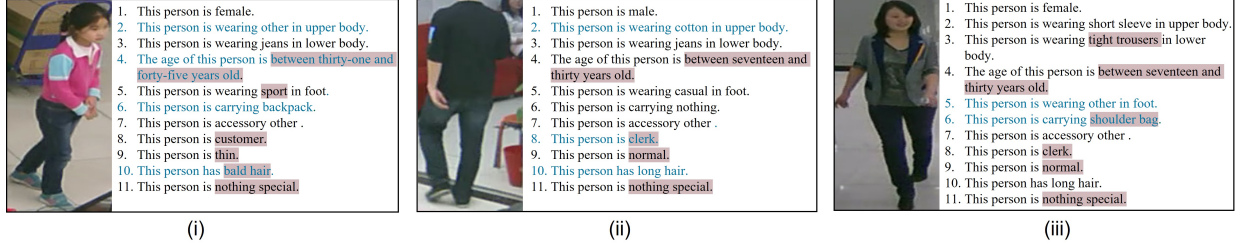


Fig. 8. Examples of image and text matching on the RAPv1 dataset.

Fig. 9. Image-to-text retrieval examples. The model is trained on the PETA dataset. Prompts with blue color indicate that the predicted text is inconsistent with ground truth. Attributes with the pink box are unseen attributes during training.

REFERENCES

- [1] Y. Zhang, Y. Jin, J. Chen, S. Kan, Y. Cen, and Q. Cao, "Pgan: Part-based nondirect coupling embedded gan for person reidentification," *IEEE MultiMedia*, vol. 27, no. 3, pp. 23–33, 2020.
- [2] S. He, H. Luo, P. Wang, F. Wang, H. Li, and W. Jiang, "Transreid: Transformer-based object re-identification," in *Proceedings of the IEEE/CVF International Conference on Computer Vision (ICCV)*, October 2021, pp. 15 013–15 022.
- [3] Y. Zhang, F. Zhang, Y. Jin, Y. Cen, V. Voronin, and S. Wan, "Local correlation ensemble with gcn based on attention features for cross-domain person re-id," *ACM Transactions on Multimedia Computing, Communications, and Applications (TOMM)*, 2022.
- [4] S. Wang, Y. Duan, H. Ding, Y.-P. Tan, K.-H. Yap, and J. Yuan, "Learning transferable human-object interaction detector with natural language supervision," in *Proceedings of the IEEE/CVF Conference on Computer Vision and Pattern Recognition (CVPR)*, June 2022, pp. 939–948.
- [5] X. Chang, P. Ren, P. Xu, Z. Li, X. Chen, and A. G. Hauptmann, "A comprehensive survey of scene graphs: Generation and application," *IEEE Transactions on Pattern Analysis and Machine Intelligence*, 2021.
- [6] C. Tang, L. Sheng, Z. Zhang, and X. Hu, "Improving pedestrian attribute recognition with weakly-supervised multi-scale attribute-specific localization," in *Proceedings of the IEEE/CVF International Conference on Computer Vision (ICCV)*, October 2019.
- [7] H. Guo, K. Zheng, X. Fan, H. Yu, and S. Wang, "Visual attention consistency under image transforms for multi-label image classification," in *Proceedings of the IEEE/CVF Conference on Computer Vision and Pattern Recognition (CVPR)*, June 2019.
- [8] P. Liu, X. Liu, J. Yan, and J. Shao, "Localization guided learning for pedestrian attribute recognition," in *British Machine Vision Conference 2018, BMVC 2018*, 2018.
- [9] X. Liu, H. Zhao, M. Tian, L. Sheng, J. Shao, S. Yi, J. Yan, and X. Wang, "Hydraplus-net: Attentive deep features for pedestrian analysis," in *Proceedings of the IEEE international conference on computer vision*, 2017, pp. 350–359.
- [10] X. Cheng, M. Jia, Q. Wang, and J. Zhang, "A simple visual-textual baseline for pedestrian attribute recognition," *IEEE Transactions on Circuits and Systems for Video Technology*, pp. 1–1, 2022.
- [11] W. Li, Z. Cao, J. Feng, J. Zhou, and J. Lu, "Label2Label: A Language Modeling Framework for Multi-Attribute Learning," *arXiv e-prints*, p. arXiv:2207.08677, Jul. 2022.
- [12] A. Radford, J. W. Kim, C. Hallacy, A. Ramesh, G. Goh, S. Agarwal, G. Sastry, A. Askell, P. Mishkin, J. Clark et al., "Learning transferable visual models from natural language supervision," in *International Conference on Machine Learning*. PMLR, 2021, pp. 8748–8763.
- [13] J. Zhu, S. Liao, D. Yi, Z. Lei, and S. Z. Li, "Multi-label cnn based pedestrian attribute learning for soft biometrics," in *2015 International Conference on Biometrics (ICB)*, 2015, pp. 535–540.
- [14] X. Zhao, L. Sang, G. Ding, Y. Guo, and X. Jin, "Grouping attribute recognition for pedestrian with joint recurrent learning," in *IJCAI*, vol. 2018, 2018, p. 27th.
- [15] J. Cao, Y. Li, and Z. Zhang, "Partially shared multi-task convolutional neural network with local constraint for face attribute learning," in *Proceedings of the IEEE Conference on Computer Vision and Pattern Recognition (CVPR)*, June 2018.

- [16] E. M. Hand and R. Chellappa, "Attributes for improved attributes: A multi-task network utilizing implicit and explicit relationships for facial attribute classification," in *Proceedings of the Thirty-First AAAI Conference on Artificial Intelligence, February 4-9, 2017, San Francisco, California, USA*, S. Singh and S. Markovitch, Eds. AAAI Press, 2017, pp. 4068–4074.
- [17] J. Jia, X. Chen, and K. Huang, "Spatial and semantic consistency regularizations for pedestrian attribute recognition," in *Proceedings of the IEEE/CVF International Conference on Computer Vision (ICCV)*, October 2021, pp. 962–971.
- [18] Z. Liu, P. Luo, S. Qiu, X. Wang, and X. Tang, "Deep-fashion: Powering robust clothes recognition and retrieval with rich annotations," in *Proceedings of the IEEE Conference on Computer Vision and Pattern Recognition (CVPR)*, June 2016.
- [19] Z. Ding, C. Ding, Z. Shao, and D. Tao, "Semantically self-aligned network for text-to-image part-aware person re-identification," *CoRR*, vol. abs/2107.12666, 2021. [Online]. Available: <https://arxiv.org/abs/2107.12666>
- [20] D. Li, X. Chen, and K. Huang, "Multi-attribute learning for pedestrian attribute recognition in surveillance scenarios," in *2015 3rd IAPR Asian Conference on Pattern Recognition (ACPR)*, 2015, pp. 111–115.
- [21] N. Sarafianos, X. Xu, and I. A. Kakadiaris, "Deep imbalanced attribute classification using visual attention aggregation," in *Proceedings of the European Conference on Computer Vision (ECCV)*, September 2018.
- [22] M. S. Sarfraz, A. Schumann, Y. Wang, and R. Stiefelhagen, "Deep view-sensitive pedestrian attribute inference in an end-to-end model," in *British Machine Vision Conference 2017, BMVC 2017, London, UK, September 4-7, 2017*. BMVA Press, 2017.
- [23] M. M. Kalayeh, B. Gong, and M. Shah, "Improving facial attribute prediction using semantic segmentation," in *Proceedings of the IEEE Conference on Computer Vision and Pattern Recognition (CVPR)*, July 2017.
- [24] W. J. Scheirer, A. de Rezende Rocha, A. Sapkota, and T. E. Boult, "Toward open set recognition," *IEEE Transactions on Pattern Analysis and Machine Intelligence*, vol. 35, no. 7, pp. 1757–1772, 2013.
- [25] P. Saranittichai, C. K. Mummadi, C. Blaiotta, M. Munoz, and V. Fischer, "Multi-attribute open set recognition," in *DAGM German Conference on Pattern Recognition*. Springer, 2022, pp. 101–115.
- [26] S. Vaze, K. Han, A. Vedaldi, and A. Zisserman, "Open-set recognition: a good closed-set classifier is all you need?" in *International Conference on Learning Representations*, 2022.
- [27] X. Gu, T.-Y. Lin, W. Kuo, and Y. Cui, "Open-vocabulary object detection via vision and language knowledge distillation," *arXiv preprint arXiv:2104.13921*, 2021.
- [28] S. Esmaeilpour, B. Liu, E. Robertson, and L. Shu, "Zero-shot out-of-distribution detection based on the pretrained model clip," in *Proceedings of the AAAI conference on artificial intelligence*, 2022.
- [29] P. Oza and V. M. Patel, "C2ae: Class conditioned auto-encoder for open-set recognition," in *Proceedings of the IEEE/CVF Conference on Computer Vision and Pattern Recognition*, 2019, pp. 2307–2316.
- [30] X. Zhao, S. Schuster, G. Sharma, Y.-H. Tsai, M. Chandraker, and Y. Wu, "Object detection with a unified label space from multiple datasets," in *European Conference on Computer Vision*. Springer, 2020, pp. 178–193.
- [31] Z. Li, L. Yao, X. Zhang, X. Wang, S. Kanhere, and H. Zhang, "Zero-shot object detection with textual descriptions," in *Proceedings of the AAAI Conference on Artificial Intelligence*, vol. 33, no. 01, 2019, pp. 8690–8697.
- [32] S. Rahman, S. Khan, and N. Barnes, "Improved visual-semantic alignment for zero-shot object detection," in *Proceedings of the AAAI Conference on Artificial Intelligence*, vol. 34, no. 07, 2020, pp. 11 932–11 939.
- [33] A. Dosovitskiy, L. Beyer, A. Kolesnikov, D. Weissenborn, X. Zhai, T. Unterthiner, M. Dehghani, M. Minderer, G. Heigold, S. Gelly *et al.*, "An image is worth 16x16 words: Transformers for image recognition at scale," *arXiv preprint arXiv:2010.11929*, 2020.
- [34] Y. Deng, P. Luo, C. C. Loy, and X. Tang, "Pedestrian attribute recognition at far distance," in *Proceedings of the 22nd ACM international conference on Multimedia*, 2014, pp. 789–792.
- [35] D. Li, X. Chen, and K. Huang, "Multi-attribute learning for pedestrian attribute recognition in surveillance scenarios," in *ACPR*, 2015, pp. 111–115.